Toward Controlling the Surface Morphology of Macroporous Copolymer Particles

Stanislav Dubinsky,[†] Jai Il Park,[†] Ilya Gourevich,[†] Carol Chan,[†] Martin Deetz,[‡] and Eugenia Kumacheva*[,†]

Department of Chemistry, University of Toronto, 80 St. George Street, Toronto, Ontario M5S 3H6, Canada, and Rohm and Haas Chemicals, LLC, 727 Norristown Road, Spring House, Pennsylvania 19477-0904

Received December 17, 2008; Revised Manuscript Received January 28, 2009

ABSTRACT: Syntheses of macroporous polymer particles under certain conditions produce microbeads with a smooth nonporous "skin" layer. This effect limits the applications of porous microbeads by preventing solute molecules to permeate the dense particle surface and reach particle's porous interior. This paper reports a straightforward method that—without the adjustment of the composition of microbeads—can be used to suppress the formation of the "skin" on the surface of macroporous polymer particles. The approach presented as a solubility parameter−interfacial tension "map" paves the way to the selection of a broader range of porogen solvents and hence better rationalization of the composition of the monomer mixtures used in the synthesis of macroporous particles.

1. Introduction

Macroporous polymer resins are a class of materials with a permanent well-defined structure comprising pores in the size range from 10 to 10 000 Å.[1,2] Macroporous polymers have a broad range of applications including their use as ion exchange resins and sorbents,[1,2] catalyst supports,[3,4] materials for biomedical applications,[5−7] and stationary phases for HPLC.[2,8] Macroporous polymer resins are exploited either as macroscopic materials (monoliths)[9−11] or as porous polymer beads[12] which are typically produced by suspension polymerization[1−3] and seed emulsion polymerization.[13,14]

One of the most common strategies used for the preparation of macroporous resins exploits free-radical copolymerization of monomers with multifunctional cross-linking agents in the presence of an inert diluent (a porogen solvent).[1−3] Since the monomer mixture is miscible with the porogen solvent, but the polymer is not, the polymerization process leads to the phase separation between the polymer and the solvent. Removing a porogen from the system yields a network of pores. The formation of macroporous resins may occur via two mechanisms which differ according to the time at which phase separation takes place, with respect to the gel point.[1] In χ-induced syneresis, phase separation in the reaction system occurs before the gel point. With increasing conversion of monomer to polymer, intramolecularly cross-linked particles (nuclei) agglomerate into larger clusters, which ultimately form a polymer network. At the end of the polymerization, the system consists of two phases: a polymer and a liquid porogen comprising a small amount of an unreacted monomer. Here χ is the polymer−solvent interaction parameter, which reflects the difference between the solubility parameters of the polymer and the porogen.[1,15] The larger the value of χ, the larger is the extent of phase separation between the porogen solvent and the polymer and hence the larger are the pores.[1,16,17] Formation of macroporous resins via ν-induced syneresis is favored by the use of better quality porogen solvents (than those used in χ-induced syneresis) and a high concentration of the cross-linker (ν refers to the degree of cross-linking of the polymer).[1,15] During the process of phase separation, either small microgel particles are formed in the continuous liquid phase (macrosyneresis) or small droplets form within the gel (microsyneresis). In either case, phase separation occurs *during* the formation of a gel, which yields smaller polymer agglomerates and hence higher specific surface area of the macroporous materials than that generated by χ-induced syneresis.[1]

A serious problem in the preparation of macroporous resins and polymer particles, in particular, is the formation of the "skin"—a thin dense surface layer with very scarce and small pores, if any. The skinning effect limits the applications of macroporous particles, since it allows only a limited number of molecules to permeate the particle surface and reach the interior of the microbeads.[18] The formation of the "skin" on the surface of macroporous particles was reported by several research groups.[4,20−25] Ford et al. synthesized macroporous copolymer beads by copolymerizing styrene, (chloromethyl) styrene, and divinylbenzene dissolved in 4-methyl-2-pentanol.[4] The authors showed that the formation of the smooth polymer "skin" with occasional small pores was favored by increasing concentration of the cross-linking agent; however, they provided no explanation for this phenomenon. Pelzbauer et al.[24] reported the formation of a dense layer of microglobules on the surface of poly(glycidyl methacrylate−ethylene dimethacrylate) macroporous particles when cyclohexanol or cyclohexanol−dodecanol porogen solvents were used.[20−24] Small pores on the surface of the particles originated from either the voids between the close-packed microglobules or the removal of low-molecular-weight molecules after extracting the porogen. In the interior of particles, polymer globules had the same size as on the microbead surface; however, they exhibited a more sparse packing. The authors ascribed the formation of the dense surface layer to the compressive action of interfacial tension between the polymer and the continuous aqueous phase. The formation of the "skin" was suppressed by tuning the composition of the monomer mixture, that is, by decreasing the concentration of the cross-linking agent, by increasing the concentration of the porogen solvent in the monomer mixture, and by reducing the content of dodecanol (poor solvent) in the porogen liquid.[19,20,22−24]

Variation in the composition of the monomer mixture affects both the surface and the internal structure of macroporous particles. For example, a decrease in the

* To whom correspondence should be addressed.
[†] University of Toronto.
[‡] Rohm and Haas Chemicals, LLC.

10.1021/ma802813v CCC: $40.75
Published on Web 02/23/2009

concentration of the cross-linking agent results in a coarser globular structure of the macroporous polymers and yields a polymer with a smaller specific surface area.[20] Therefore, the next-step optimization of the formulation may be required, in order to fine-tune the distribution of pore sizes in the ultimate material. A more attractive approach would exploit the modification of the continuous phase, which would allow one to suppress the formation of the "skin" without losing control of the internal structure of the particles. To the best of our knowledge, this approach has not yet been reported.

In the present work, we used two methods to suppress the formation of the "skin" layer on the surface of macroporous particles. We hypothesized that the formation of the "skin" occurs due to competitive interactions of the polymer and monomer−solvent phases with a continuous phase. When the value of interfacial tension, γ_{12}, between the continuous phase and the monomer−solvent phase is substantially higher than γ_{12} between the polymer and the continuous phase, the interface is deprived of the monomer−solvent mixture, which is squeezed out to the particle interior. Therefore, in an aqueous continuous phase, the utilization of strongly nonpolar porogens would favor the formation of the "skin".[24,26,27] For slowly polymerizing systems, the compressive action of the interfacial tension between the forming polymer and the continuous aqueous phase may provide an additional factor in the formation of "skin".[19,20,22−24]

We suppressed the formation of the "skin" on the surface of poly(glycidyl methacrylate−ethylene dimethacrylate) (poly(GMA−EGDMA)) particles by reducing the value of γ_{12} between the monomer mixture and the continuous aqueous phase in two ways: (i) by introducing a surfactant in the continuous phase and (ii) by adjusting the polarity of the continuous aqueous phase. We note that in our previous work on the microfluidic synthesis of macroporous particles[17] the formation of the "skin" on the surface of microbeads was not prominent; however, a scaled-up multihour polymerization process revealed that a fraction of the particles synthesized using dioctyl phthalate and diisodecyl phthalate had a smooth "skinned" surface.

We demonstrated the feasibility of our approaches by using semicontinuous microfluidic photopolymerization of macroporous polymer particles. Microfluidic synthesis not only allows highly reproducible production of particles with precisely controlled dimensions[28−30] but also yields microbeads with enhanced control of their internal structure.[17,30]

For the system studied, we report the critical values of solubility parameters of the porogen solvents and the values of γ_{12} that favor the formation of the skin. As a result of our work, we present a "map" plotted in the interfacial tension−solubility parameter space, which provides guidance to the synthesis of "skin"-free macroporous particles.

2. Experimental Section

Materials. Monomers glycidyl methacrylate (GMA) and ethylene glycol dimethacrylate (EGDMA), photoinitiator 2,2-dimethoxy-2-phenylacetophenone (DMPA), a stabilizer poly(vinyl alcohol) (PVA, Sigma-Aldrich, 87−89% hydrolyzed, M_w = 13 000−23 000), surfactants Triton X-100, 1-decanesulfonic acid, sodium salt 98%, and sodium dodecyl sulfate (SDS), tetrahydrofuran (THF), and the porogens diethyl phthalate, diisobutyl phthalate, dioctyl phthalate, and diisodecyl phthalate were purchased from Aldrich Canada and used as received. The surfactant Aerosol MA 80-I was supplied by Cytec Industries Inc. Photoresist SU-8 was purchased from MicroChem. Prepolymer Sylgard 184 Silicon Elastomer kit was received from Dow Corning Corp. Polyethylene tubing was purchased from Becton Dickinson.

Solubility Parameters of Porogen Solvents. We used diethyl phthalate (DEP), diisobutyl phthalate (DBP), dioctyl phthalate (DOP), diisodecyl phthalate (DDP), and mixtures of DBP and DOP as porogen solvents. Table 1 shows the values of solubility parameters of the porogens, comonomers GMA and EGDMA, and poly(GMA−EGDMA). For DBP and DOP mixed in volumetric ratios of 3:1, 1:1, and 1:3, respectively, the solubility parameter, δ_{mix}, was determined as $\delta_{mix} = \varphi_{DBP}\delta_{DBP} + \varphi_{DOP}\delta_{DOP}$,[27] where δ_{DBP} and δ_{DOP} are the solubility parameters and φ_{DBP} and φ_{DOP} are the volume fractions of DBP and DOP, respectively.

Table 1. Solubility Parameters of the Porogen Solvents, the Comonomers, and the Corresponding Polymer

chemicals	solubility parameter, $(MPa)^{1/2}$
DEP	20.5[27]
DBP	19.0[27]
DBP/DOP 3:1 (v/v)	18.3
DBP/DOP 1:1 (v/v)	17.6
DBP/DOP 1:3 (v/v)	16.9
DOP	16.2[27]
DDP	14.7[27]
GMA	18.2[31]
EGDMA	18.2[32]
poly(GMA-*co*-EGDMA)	24.0[17]

Measurement of Interfacial Tension. The value of interfacial tension, γ_{12}, between the continuous aqueous phase and the monomer phase (a mixture of GMA, EGDMA, a porogen solvent, and a photoinitiator DMPA) was determined by the pendant droplet method using a tensiometer (DSA100, Kruss). A droplet of the monomer−porogen mixture used in the synthesis of particles was immersed into the 2.5 wt % aqueous solution of PVA containing various concentrations of surfactants or THF.

Microfluidic Synthesis. A microfluidic reactor for the synthesis of macroporous particles was fabricated in poly(dimethylsiloxane) by the soft-lithography method.[33] A mixture containing 27 vol % GMA, 18 vol % EGDMA, and 55 vol % of the porogen solvent (later in the text referred to as a "monomer mixture") was emulsified in the microfluidic flow-focusing droplet generator.[34] The flow rate of the monomer mixture and the continuous phase were 0.3 and 6.0 mL/h, respectively. A photoinitiator DMPA was introduced in this mixture to the concentration of 1 wt % (based on the total content of monomers). To initiate photopolymerization of the monomers, droplets of the monomer mixture flowing through the downstream channel were exposed to UV-irradiation (I = 6 mW/cm^2, Bluepoint 3, Hohle UV Technology) for ca. 60 s. The design of the microfluidic reactor comprising an emulsification and a polymerization compartments is described elsewhere.[17] The reactor was placed into the cooling water bath at a temperature of 12 °C. The distance between the UV source and the microfluidic reactor was ca. 10 cm. Following on-chip polymerization, the particles were transferred into the 250 mL glass stirred reactor and postpolymerized under UV-irradiation for another 180 s (I = 200 mW/cm^2, Hohle UV Technology). The distance between the UV source and the glass reactor was ca. 5 cm. Following postpolymerization, the porogen liquids were removed by washing the microbeads in methanol and acetone. By imaging polymer particles before and after postpolymerization, we ensured that the structure of particles was controlled by their on-chip polymerization in the microfluidic reactor and that postpolymerization did not change their surface structure.

Particle Characterization. The surface morphology and the internal structure of macroporous poly(GMA−EGDMA) particles were examined by scanning electron microscopy (Hitachi S-5200) at the accelerating voltage of 1 kV. A droplet of the dispersion of particles in methanol was placed onto the glass slide and allowed to dry. The dry sample particles were attached to the aluminum sample holder using a graphite conductive adhesive (EMS). In order to image the internal structure of the macroporous particles, they were frozen in liquid nitrogen and microtomed with a glass knife.

The average size of globules and pores on the surface of the macroporous particles was obtained by image analysis software Image Tool (The University of Texas, San Antonio) and was based on the analysis of 50 particles.

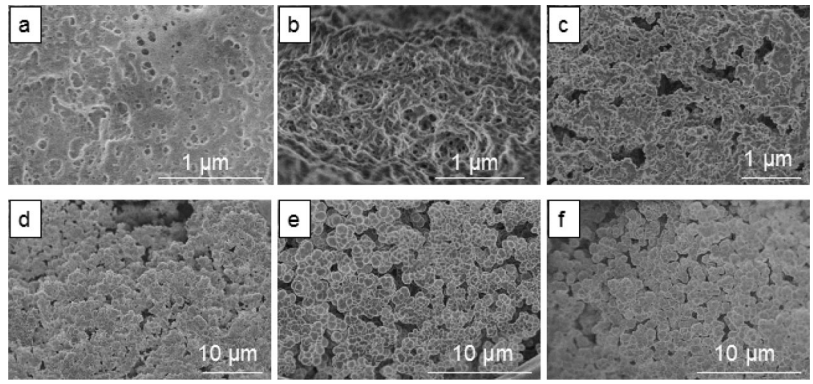

Figure 1. Typical SEM images of the internal structure of macroporous poly(GMA−EGDMA) particles, synthesized in the presence of (a) DEP, (b) DBP, (c) DBP/DOP 3:1 (v/v), (d) DBP/DOP 1:1 (v/v), (e) DOP, and (f) DDP.

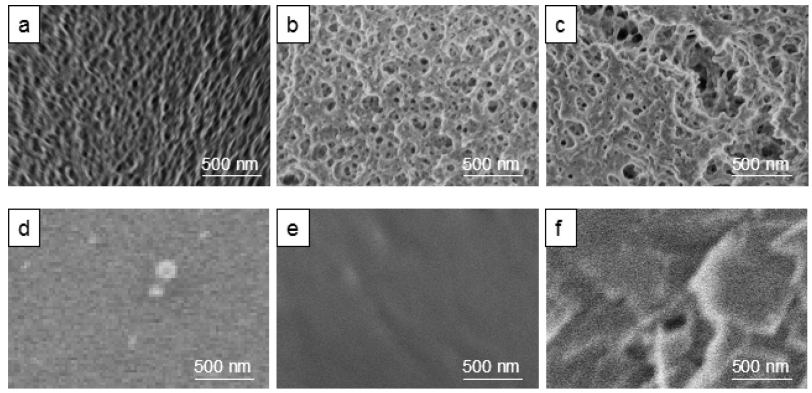

Figure 2. SEM images of the surface of poly(GMA-*co*-EGDMA) macroporous particles, synthesized from the monomer mixture in the presence of (a) DEP, (b) DBP, (c) DBP/DOP 3:1 (v/v), (d) DBP/DOP 1:1 (v/v), (e) DOP, and (f) DDP.

3. Results and Discussion

Figure 1 shows the internal structure of the macroporous particles synthesized by copolymerizing GMA and EGDMA in the presence of various porogen liquids and their mixtures. With reducing values of solubility parameters of the porogens (that is, with increasing difference between the solubility parameters of the porogens and poly(GMA−EGDMA) (see Table 1)), the size of pores in the particles increased. Particles derived from the droplets comprising DEP, DBP, and DBP/DOP 3:1 (v/v) (the value of δ above 17.6 $MPa^{1/2}$) had noticeably smaller pores than other microbeads, presumably due to the dominant role of ν-induced syneresis.[1,15] For the particles synthesized in the presence of DBP/DOP 1:1 (v/v), DOP, and DDP, χ-induced syneresis was most probably the mechanism of pore formation.[1,15] Phase separation occurring before the gel point facilitated the formation of large polymer clusters and the formation of a structure with a larger size of pores.[1]

Figure 2 shows representative SEM images of the surfaces of polymer particles shown in Figure 1. The particles featured two types of surface morphologies. The microbeads generated from the monomer mixture comprising DEP, DBP, and DBP/DOP 3:1 (v/v) had a porous surface structure (Figure 2a−c). Based on the image analysis, the size of pores was ca. 60−114 nm. In contrast, particles synthesized from the monomer mixture containing DBP/DOP 1:1 (v/v), DOP, and DDP featured a smooth surface (Figure 2d−f). The surface of the particles synthesized with DDP (Figure 2f) had a "flaky" structure with tiny pores of ca. 90 nm.

Figure 3 allows SEM images of an individual porous particle coated with a "skin", which was synthesized using a DBP/DOP 1:1 (v/v) mixture as a porogen. The surface of the particle was covered with a 1−2 μm thick smooth layer of the polymer;

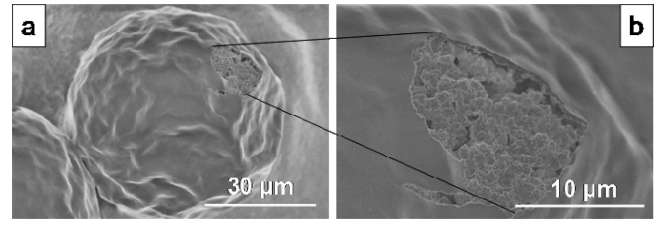

Figure 3. SEM images of the macroporous poly(GMA−EGDMA) particle, synthesized in the presence of DBP/DOP 1:1 (v/v) porogen: (a) an individual microsphere; (b) a zoomed-in image of the surface of the particles beneath the "skin".

however, the interior of the particle featured a well-defined porous structure (Figure 3b).

To examine the relation between the surface and the bulk structure of polymer particles, we examined the variation in the interfacial tension between continuous aqueous phase and monomer mixtures containing different porogens (and, hence, possessing different solubility parameters). In Figure 4, the value of γ_{12} reduced from ca. 7.5 mN/m (for the monomer mixture comprising DDP) to ca. 1.5 mN/m (for the mixture of monomers with DEP), featuring an inflection in the trend for $\delta > 18$ $MPa^{1/2}$. This graph presents a "map" plotted in the $\gamma_{12}-\delta$ space and provides guidance to the synthesis of "skin"-free particles. The vertical dashed line gives the threshold value of δ for the porogens used in the synthesis of porous poly(GMA−EGDMA) particles in the continuous aqueous phase. More importantly, the horizontal dashed line shows that particles with a porous surface structure are synthesized when the value of γ_{12} between the monomer mixture and an aqueous continuous phase is below ca. 3.5 mN/m.

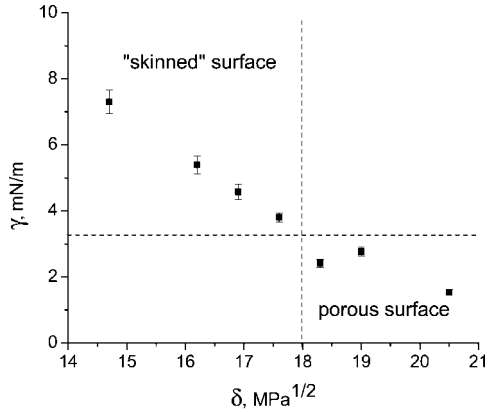

Figure 4. Variation in interfacial tension, γ_{12}, between the 2.5 wt % aqueous solution of PVA (the carier phase) and the monomer phase comprising different porogen solvents, plotted as a function of the solubility parameter of the porogens.

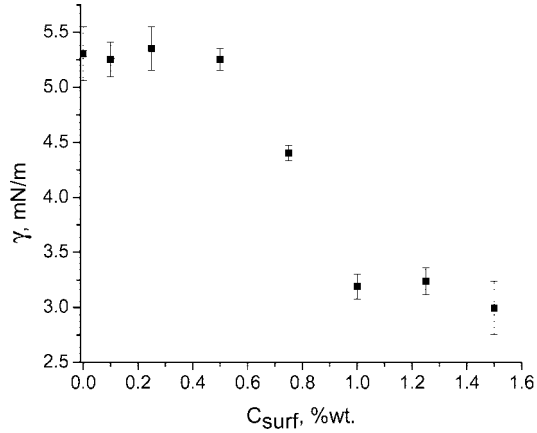

Figure 5. Variation in interfacial tension, γ_{12}, between the monomer mixture comprising GMA, EGDMA, and DOP and an aqueous solution of 2.5 wt % of PVA and Triton X-100, plotted versus the concentration of Triton X-100, C_{surf}.

On the basis of the results shown in Figures 1−4, we conclude that while the variation in solubility parameters of the porogens can be used to control the internal porous structure of polymer particles, the formation of the "skin" does not allow the exploitation of porogen solvents with relatively low solubility parameters.

We addressed this challenge by reducing the value of interfacial tension between the continuous phase and the monomer mixture. In contrast to the approaches developed by other groups,[4,19−21,24] we did not change the composition of monomer mixture and varied the composition of the continuous phase only. As an exemplary system, we used the monomer mixture containing DOP, the porogen solvent with a low value of δ and thus one of the least favorable for the formation of particles with a porous surface structure.

In the first series of experiments, we reduced the value of interfacial tension between the monomer mixture and the continuous phase (a 2.5 wt % aqueous solution of PVA) by adding a surfactant into the continuous phase. Among the range of surfactants studied, including Triton X-100, 1-decanesulfonic acid, sodium dodecyl sulfate, and Aerosol MA 80-I, Triton X-100 provided the strongest reduction in γ_{12}, and hence it was chosen for further studies.

Figure 5 shows the variation in γ_{12} between the droplet of monomer−DOP mixture and the 2.5 wt % aqueous solution of PVA, containing different amounts of Triton X-100. As expected, the value of γ_{12} decreased with increasing concentration of the surfactant, C_{surf}, with a particularly strong reduction occurring at 0.5 wt % $\leq C_{surf} \leq$ 1.0 wt %. For $C_{surf} \geq 1$, the value of γ_{12} of ca. 3.0 mN/m leveled off. Two important features follow from Figure 5. First, the value of $C_{surf} \approx 1.0$ wt % substantially exceeded the critical concentration of micellization of Triton X-100 in water of 0.015 wt %,[35] which suggested strong interactions between Triton X-100 and PVA. Second, the value of γ_{12} of ca. 3.0 mN/m was very close to the threshold value of interfacial tension at which the particles with a porous surface were formed (Figure 2c).

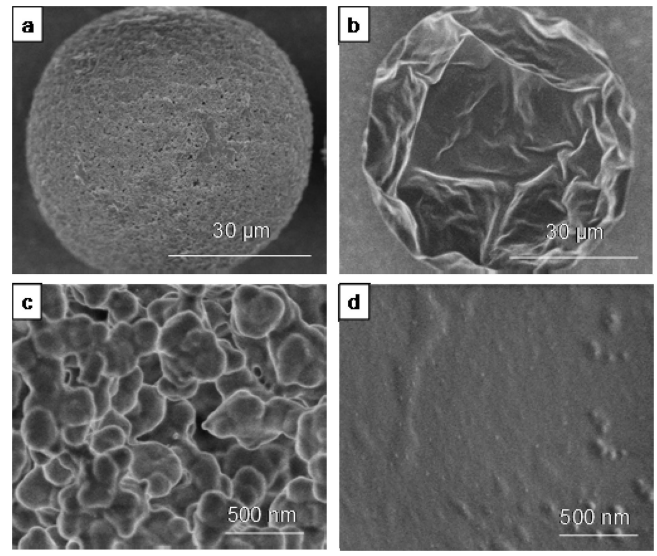

Figure 6. Typical SEM images of poly(GMA−EGDMA) particles synthesized in the presence of DOP porogen in the continuous phase comprising 2.5 wt % PVA and Triton X-100 at concentration 1 wt % (a, c) and 0.5 wt % (b, d). Images (a, b) show individual microspheres. Images (c, d) show a detailed surface morphology of the macroporous particles under high magnification.

To utilize the second feature in the synthesis of macroporous particles, we emulsified a mixture of comonomers with DOP in the continuous aqueous phase containing 2.5 wt % of PVA and Triton X-100 at the concentration 0.5 or 1.0 wt %. Figure 6 shows that at $C_{surf} = 1$ wt % the particles had a well-defined porous surface structure. The surface featured close-packed polymer microglobules with dimensions from 100 to 300 nm and the mean size of pores of ca. 200 nm (Figure 6c). This surface morphology was similar to the internal morphology of the macroporous particles synthesized with DOP in the absence of Triton X-100 (Figure 1e). In contrast, the particles synthesized at $C_{surf} = 0.5$ wt % had a smooth surface, analogous to that of the particles prepared without the surfactant (Figure 6b,d).

Our hypothesis was further tested in the second series of experiments in which the value of interfacial tension between the monomer mixture and the continuous phase was reduced by mixing a 2.5 wt % aqueous solution of PVA with tetrahydrofuran (THF), that is, by decreasing the polarity of the continuous phase. The threshold value of γ_{12} of ca. 3.0 mN/m was obtained by introducing THF in the aqueous solution in the 22:78 (v/v) ratio. Since THF swells PDMS used for the fabrication of the reactor,[36] only emulsification was conducted in the microfluidic droplet generator, whereas photopolymerization of the monomer mixture was carried out in the stirred glass flask. Figure 7 shows that particles synthesized in the THF−water continuous phase had a well-defined porous surface structure. The surface featured close-packed microglobules with dimensions from 50 to 100 nm and the size of pores in the range from ca. 50 to 80 nm (Figure 7b). The smaller size of globules than in experiments using the surfactant Triton X-100 was presumably caused by partial dissolution of the monomer

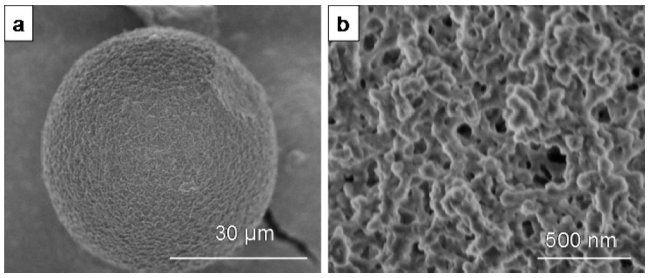

Figure 7. Typical SEM images of poly(GMA−EGDMA) particles synthesized in the presence of DOP porogen in the continuous phase comprising 2.5 wt % PVA and THF at concentration 20 wt %. Image (a) shows individual microsphere, and image (b) shows a detailed surface morphology of the macroporous particle.

mixture in THF−water solvent; nevertheless, we believe that on the time scale of experiments the suppressed "skinning" was caused by the reduction in interfacial tension.

4. Conclusions

To summarize, our work shows a straightforward method that can be used to suppress the formation of the "skin" on the surface of macroporous polymer particles. The "map" plotted in the $\delta-\gamma_{12}$ space paves the way to rationalization of the composition of the monomer mixtures and the selection of a broader range of porogen solvents. In particular, for the particles synthesized in our work, the presence of pendant epoxide groups allows subsequent surface modification of the microbeads,[25] whereas a well-defined porous surface structure of the particles makes them permeable for large molecules. Although we show two methods that can prevent the formation of the skin on the particle surface, the use of surfactants has obvious advantages in comparison with introduction of organic solvents in the continuous phase. Microfluidic synthesis provides the ability to tune the size of microbeads by varying the flow rates of liquids, to synthesize particles with narrow polydispersity, and to conduct photopolymerization under well-defined conditions; however, the applicability of the method would depend on the increased productivity of microfluidic synthesis in multiple parallel reactors.[37−39]

Acknowledgment. The authors thank Rohm and Haas Chemicals and Materials Manufacturing Ontario for financial support of this research.

References and Notes

(1) Okay, O. *Prog. Polym. Sci.* **2000**, *25*, 711–779.
(2) Seidl, J.; Malinsky, J.; Dusek, K.; Heitz, W. *Adv. Polym. Sci.* **1967**, *5*, 113–213.
(3) Sherrington, D. C. *Chem. Commun.* **1998**, 2275–2286.
(4) Ford, W. T.; Lee, J.; Tomoi, M. *Macromolecules* **1982**, *15*, 1246–1251.
(5) Horak, D.; Lednicky, F.; Rehak, V.; Svec, F. *J. Appl. Polym. Sci.* **1993**, *49*, 2041–2050.
(6) Paredes, B.; Gonzalez, S.; Rendueles, M.; Diaz, J. M. *Sep. Purif. Technol.* **2004**, *40*, 243–250.
(7) Stegmayr, B. *Transfus. Apher. Sci.* **2005**, *32*, 209–220.
(8) Benes, M. J.; Horak, D.; Svec, F. *J. Sep. Sci.* **2005**, *28*, 1855–1875.
(9) (a) Svec, F.; Frechet, J. M. J. *Anal. Chem.* **1992**, *54*, 820–822. (b) Svec, F.; Frechet, J. M. J. *Chem. Mater.* **1995**, *7*, 707–715. (c) Peters, E. C.; Svec, F.; Frechet, J. M. J. *Adv. Mater.* **1999**, *11*, 1169–1181.
(10) Rohr, T.; Yu, C.; Davey, M.; Svec, F.; Frechet, J. M. J. *Electrophoresis* **2001**, *22*, 3959–3967.
(11) Janco, M.; Xie, S. F.; Peterson, D. S.; Allington, R. W.; Svec, F.; Frechet, J. M. J. *J. Sep. Sci.* **2002**, *25*, 909–916.
(12) Guiochon, G. *J. Chromatogr. A* **2007**, *1168*, 101–168.
(13) Ugelstad, J.; Kaggerud, K. H.; Hansen, F. K.; Berge, A. *Makromol.Chem.* **1979**, *180*, 737–744.
(14) Ugelstad, J.; Söderberg, L.; Berge, A.; Bergström, J. *Nature (London)* **1983**, *303*, 95–96.
(15) Dušek, K. In *Polymer Networks: Structure and Mechanical Properties*; Chompff, A. J., Newman, S., Eds.; Plenum Press: New York, 1971; p 245.
(16) Zaidi, S. A. R.; Shah, G. B. *Macromol. Chem. Phys.* **2000**, *201*, 2760–2764.
(17) Dubinsky, S.; Zhang, H.; Nie, Z. H.; Gourevich, I.; Voicu, D.; Deetz, M.; Kumacheva, E. *Macromolecules* **2008**, *41*, 3555–3561.
(18) Benson, J. R. *Am. Lab.* **2003**, *35*, 44–49.
(19) Horak, D.; Svec, F.; Ribeiro, C. M. A.; Kalal, J. *Angew. Makromol. Chem.* **1980**, *87*, 127–136.
(20) Horak, D.; Pelzbauer, Z.; Bleha, M.; Ilavsky, M.; Svec, F.; Kalal, J. *J. Appl. Polym. Sci.* **1981**, *26*, 411–421.
(21) Horak, D.; Pelzbauer, Z.; Svec, F.; Kalal, J. *J. Appl. Polym. Sci.* **1981**, *26*, 3205–3211.
(22) Horak, D.; Svec, F.; Bleha, M.; Kalal, J. *Angew. Makromol. Chem.* **1981**, *95*, 109–115.
(23) Horak, D.; Svec, F.; Ilavsky, M.; Bleha, M.; Baldrian, J.; Kalal, J. *Angew. Makromol. Chem.* **1981**, *95*, 117–127.
(24) Pelzbauer, Z.; Lukas, J.; Svec, F.; Kalal, J. *J. Chromatogr.* **1979**, *171*, 101–107.
(25) Svec, F.; Hradil, J.; Coupek, J.; Kalal, J. *Angew. Makromol. Chem.* **1975**, *48*, 135–143.
(26) Yuan, H. G.; Kalfas, G.; Ray, W. H. *J. Macromol. Sci., Rev. Macromol. Chem. Phys.* **1991**, *C31*, 215–299.
(27) *CRC Handbook of Solubility Parameters and Other Cohesion Parameters*, 4th ed.; Barton, A. F. M., Ed.; CRC Press: Boca Raton, FL, 1988; p 62.
(28) (a) Seo, M.; Nie, Z.; Xu, S.; Mok, M.; Lewis, P. C.; Graham, R.; Kumacheva, E. *Langmuir* **2005**, *21*, 11614–11622. (b) Xu, S.; Nie, Z.; Seo, M.; Lewis, P.; Kumacheva, E.; Stone, H. A.; Garstecki, P.; Weibel, D. B.; Gutlin, I.; Whitesides, G. M. *Angew.Chem., Int. Ed.* **2005**, *44*, 724–728. (c) Lewis, P. C.; Graham, R.; Xu, S.; Nie, Z.; Seo, M.; Kumacheva, E. *Macromolecules* **2005**, *38*, 4536–4538.
(29) Dendukuri, D.; Tsoi, K.; Hatton, T. A.; Doyle, P. S. *Langmuir* **2005**, *21*, 2112–2116.
(30) Li, W.; Pham, H. H.; Nie, Z.; MacDonald, B.; Guenther, A.; Kumacheva, E. *J. Am. Chem. Soc.* **2008**, *130*, 9935–9941.
(31) Yang, W.; Hu, J.; Tao, Z.; Li, L.; Wang, C.; Fu, S. *Colloid Polym. Sci.* **1999**, *277*, 446–451.
(32) Fang, D.; Pan, Q.; Rempel, G. L. *J. Appl. Polym. Sci.* **2007**, *103*, 707–715.
(33) Xia, Y.; Whitesides, G. M. *Annu. Rev. Mater. Sci.* **1998**, *28*, 153–184.
(34) Anna, S. L.; Bontoux, N.; Stone, H. A. *Appl. Phys. Lett.* **2003**, *82*, 364–366.
(35) Tiller, G. E.; Mueller, T. J.; Dockter, M. E.; Struve, W. G. *Anal. Biochem.* **1984**, *141*, 262–266.
(36) Lee, J. N.; Park, C.; Whitesides, G. M. *Anal. Chem.* **2003**, *75*, 6544–6554.
(37) Li, W.; Nie, Z.; Zhang, H.; Paquet, C.; Seo, M.; Garstecki, P.; Kumacheva, E. *Langmuir* **2007**, *23*, 8010–8014.
(38) Li, W.; Young, L.; Nie, Z.; Seo, M.; Garstecki, P.; Simon, C.; Kumacheva, E. *Soft Matter* **2008**, *4*, 258–262.
(39) Nisisako, T.; Torii, T.; Takahashi, T.; Takizawa, Y. *Adv. Mater.* **2006**, *18*, 1152–1156.

MA802813V